Video Article

Benefits of Cardiac Resynchronization Therapy in an Asynchronous Heart Failure Model Induced by Left Bundle Branch Ablation and Rapid Pacing

Jingfeng Wang*[1], Zhenning Nie*[1], Haiyan Chen*[2], Xianhong Shu[2], Zhaohua Yang[3], Ruiming Yao[1], Yangang Su[1], Junbo Ge[1]

[1]Department of Cardiology, Shanghai Institute of Cardiovascular Diseases, Zhongshan Hospital, Fudan University

[2]Department of Echocardiography, Shanghai Institute of Medical imaging, Shanghai Institute of Cardiovascular Diseases, Zhongshan Hospital, Fudan University

[3]Department of Cardiac surgery, Shanghai Institute of Cardiovascular Diseases, Zhongshan Hospital, Fudan University

*These authors contributed equally

Correspondence to: Yangang Su at su.yangang@zs-hospital.sh.cn

URL: https://www.jove.com/video/56439
DOI: doi:10.3791/56439

Keywords: Medicine, Issue 130, Cardiac resynchronization therapy, asynchronous, heart failure, reverse remodeling, left bundle branch block, left bundle branch ablation, rapid pacing, strain, speckle tracking imaging, aortic velocity time integral

Date Published: 12/11/2017

Citation: Wang, J., Nie, Z., Chen, H., Shu, X., Yang, Z., Yao, R., Su, Y., Ge, J. Benefits of Cardiac Resynchronization Therapy in an Asynchronous Heart Failure Model Induced by Left Bundle Branch Ablation and Rapid Pacing. *J. Vis. Exp.* (130), e56439, doi:10.3791/56439 (2017).

Abstract

It is now well recognized that heart failure (HF) patients with left bundle branch block (LBBB) derive substantial clinical benefits from cardiac resynchronization therapy (CRT), and LBBB has become one of the important predictors for CRT response. The conventional tachypacing-induced HF model has several major limitations, including absence of stable LBBB and rapid reversal of left ventricular (LV) dysfunction after cessation of pacing. Hence, it is essential to establish an optimal model of chronic HF with isolated LBBB for studying CRT benefits. In the present study, a canine model of asynchronous HF induced by left bundle branch (LBB) ablation and 4 weeks of rapid right ventricular (RV) pacing is established. The RV and right atrial (RA) pacing electrodes via the jugular vein approach, together with an epicardial LV pacing electrode, were implanted for CRT performance. Presented here are the detailed protocols of radiofrequency (RF) catheter ablation, pacing leads implantation, and rapid pacing strategy. Intracardiac and surface electrograms during operation were also provided for a better understanding of LBB ablation. Two-dimensional speckle tracking imaging and aortic velocity time integral (aVTI) were acquired to validate the chronic stable HF model with LV asynchrony and CRT benefits. By coordinating ventricular activation and contraction, CRT uniformed the LV mechanical work and restored LV pump function, which was followed by reversal of LV dilation. Moreover, the histopathological study revealed a significant restoration of cardiomyocyte diameter and collagen volume fraction (CVF) after CRT performance, indicating a histologic and cellular reverse remodeling elicited by CRT. In this report, we described a feasible and valid method to develop a chronic asynchronous HF model, which was suitable for studying structural and biologic reverse remodeling following CRT.

Video Link

The video component of this article can be found at https://www.jove.com/video/56439/

Introduction

Advanced chronic HF is a leading cause of mortality for various cardiovascular diseases. A subset of patients with congestive heart failure (CHF) also develop ventricular conduction discoordination that aggravates symptoms and prognosis. CRT, also referred to as biventricular pacing, has been introduced as an alternative therapy for these patients for over 20 years[1,2]. Unfortunately, about 20-40% of the patients show poor response to CRT. Since then, many studies have been carried out in order to maximize CRT response[3]. It is now well recognized that patients with LBBB could benefit more from CRT than those with non-LBBB[4], since an LBBB pattern causes a larger magnitude of cardiac dyssynchrony due to asymmetry in the freedom of wall movement between septal and lateral walls. Meanwhile recent studies have begun exploring changes in gene expression and molecular remodeling associated with CRT[5]. Accompanying the structural reverse remodeling induced by CRT, cellular and molecular reversion to a normal level is of great interest[6]. Hence, it is essential to establish an optimal model of CHF with isolated LBBB for studying CRT benefits.

Chronic, rapid ventricular pacing was once used to produce CHF in a canine model. RV pacing could undoubtedly produce delayed LV contraction as a model of the LBBB-like contraction pattern. However, this type of functional asynchrony with an intact conduction system may not emulate anatomical LBBB and is not considered an appropriate model for studying CRT performance, the essence of which is to coordinate impaired electrical activation and myocardial contraction. Rapid restoration of LV contractility and partial recovery of LV dimensions after cessation of pacing were also reported[7].

Experimental studies have induced chronic LBBB by RF ablation to establish asynchronous ventricular contraction[8]. A combination of reduction in global pump function and regional invalid mechanical work could exacerbate CHF by generating cardiac inefficiency as well as cardiac remodeling at the tissue, cellular, and molecular levels. In LBBB hearts, workload is lowest in the septum and highest in the LV lateral wall. As a consequence, cardiac remodeling is most pronounced in the lateral wall[9]. The purpose of the present study is: (i) to advance a stable

Copyright © 2017 Journal of Visualized Experiments

and chronic HF model with interventricular and intraventricular mechanical asynchrony by means of rapid RV pacing in combination with LBB ablation; (ii) to confirm dyssynchronous HF in our model and CRT benefits in coordinating contraction by two-dimensional speckle tracking echocardiography and aVTI; and (iii) to preliminarily explore cellular reverse remodeling elicited by CRT.

Protocol

Fifteen male beagle dogs (12 to 18 months old, weighing around 10.0-12.0 kg) were purchased and subjected to experiments. All procedures were performed in compliance with the Guide for the Care and Use of Laboratory Animals published by the US National Institutes of Health (Publication No. 85-23, revised 1996) and were approved by the Animal Care Committee in Zhongshan Hospital, Fudan University. **Figure 1** shows the schematic workflow for all protocol steps.

1. Pre-surgery Preparation and Baseline Data Collection

1. Shave the hair of one hindlimb for venipuncture. Establish a venous access through the lateral branch of small saphenous vein of experimental beagle dogs using a venous catheter (22 G, 0.9 mm × 25 mm). Inject sodium pentobarbital (30 mg/kg) slowly via the venous catheter to induce anesthesia, which is confirmed by loss of eyelash reflex. Give additional sodium pentobarbital at the dosage of 10 mg/kg in case of anesthesia recovery during the surgery.
2. Secure the limbs to the operation table with coarse rope and keep the animal in a supine position.
3. Clip the hair of the limb extremities and chest. Paste the limb lead electrodes to limb extremities and the precordial lead electrodes at six designated locations on the chest wall. Record the baseline electrocardiogram (ECG).
4. **Echocardiographic assessment**
    1. Paste the lead electrodes of the echocardiograph to the limbs of the animal.
    2. Carry out a standard echocardiographic examination. From the conventional apical four chamber (A4C) and apical two chamber (A2C) views, obtain the LV end-diastolic volume (LVEDV), LV end-systolic volume (LVESV), and LV ejection fraction (LVEF) calculated using the biplane Simpson's method.
    3. Assess LV longitudinal strain by two-dimensional speckle tracking imaging. Perform speckle tracking on the A4C, A2C, and apical long axis view (APLAX).
    4. Obtain the longitudinal strain curves from the above three apical views at the basal, mid-ventricular, and apical levels in each wall (A4C: septum and lateral wall; A2C: anterior wall and inferior wall; APLAX: anterior-septum and posterior wall). The software will automatically integrate these data to produce a bull's eye map of 17-segment, including 6 segments at the basal level (septum, lateral wall, anterior wall, inferior wall, anterior-septum, and posterior wall), 6 segments at the mid-ventricular level (septum, lateral wall, anterior wall, inferior wall, anterior-septum, and posterior wall), 4 segments at the apical level (septum, lateral wall, anterior wall, inferior wall), and one apical cap.
    5. Time to peak strain (TTP) is defined as the time interval from the beginning of QRS complex to the lowest point of strain curve, which indicates the maximum longitudinal strain. Calculate the standard deviation of the 17-segment TTP (PSD) to evaluate the LV mechanical synchronism.
    6. Record the transaortic Doppler flow velocities in the apical five chamber view. Measure and average the aVTI in 3-4 consecutive beats.
5. **Orotracheal intubation and mechanical ventilation**
    1. Gently pull out the tongue and maintain extension of the tongue in preparation for orotracheal intubation. Position the animal in a "sniffing" position.
    2. Slowly advance the curved blade of the laryngoscope until the tip of the blade positioned between the base of the tongue and the epiglottis. Lift the laryngoscope upward to expose the vocal cords. Insert an endotracheal tube into the mouth and pass the tube beyond the vocal cords. Secure the tube to the animal head using adhesive tape.
    3. Auscultate both lungs to confirm proper endotracheal tube placement as evidenced by bilateral and symmetrical breath sounds during positive-pressure ventilation.
    4. Connect the outer end of endotracheal tube to a volume cycled respirator. Start and maintain auxiliary mechanical ventilation with room air. Set the breathing frequency at 8-20 times per min with a tidal volume at 8-15 mL/kg. Set the parameters according to SpO_2 measured by pulse oximetry.

2. Epicardial LV Pacing Electrode Implantation

1. Connect the cardiac defibrillator/monitor lead wires to the skin electrodes, which are attached to the limbs. Pre-medicate the animal with 0.3 g levofloxacin intravenously guttae.
2. After shaving the hair of the neck and chest, sterilize the anterior thoracic region and left cervical region with iodophor and pave the sterile sheets.
3. **Thoracotomy**
    1. Perform the muscle-sparing thoracotomy in a right lateral decubitus position. After administering fentanyl by a continuous rate infusion (0.01 mg/kg/hr) intravenously, incise the skin transversely from the left parasternal line at the fourth intercostal space.
    2. After blunt dissection of the 3 layers of thoracic muscle (pectoralis major, pectoralis minor, intercostals), open the left pleural cavity at the fourth intercostal space (between the 4^{th} and 5^{th} ribs) by sharp dissection. Place a rib retractor into the intercostal space. Pack sterile gauze immersed in 0.9% NaCl around the lung lobes to protect the lungs and to keep a clear field of vision.
    3. Carefully incise the lateral pericardium using electrocautery. Open the pericardium to fully expose the LV lateral wall with stay sutures (0-suture).
4. **LV pacing electrode implantation**

1. Suture the unipolar LV pacing electrode to the myocardium on the LV lateral wall with one stitch using a 4-0 suture. Make a gentle knot on the suture to prevent lacerating the myocardial tissues.
2. Connect the terminal metal pin of the pacing lead to a bridging cable to test lead parameters. After satisfactory lead parameters are achieved with the pacing threshold <2.0 V at 0.48 ms and lead impedance <2,000 Ω, slightly pull the electrode lead to guarantee a firm fixation.

5. Remove the stay sutures and carefully examine the surgery area to eliminate active bleeding.
6. Close the pericardium with two stitches using 2-0/T sutures. Remove the stuffed gauze and the rib retractor.
7. Use two pericostal sutures (0-suture) to approximate the 4^{th} and 5^{th} ribs. Close the intercostal fascia with several stitches using 2-0/T sutures. Inflate the lungs adequately using an auxiliary balloon via orotracheal intubation before the last suture. Look through the intercostals to confirm normal expansion of the lungs.
8. Reposition the muscle layers back in place with no sutures. The pacing lead penetrates the pericardium, intercostal fascia, and muscle layers successively through the gap between surgery knots.
9. Incise the skin of the left cervical region and dissect the subcutaneous tissue until reaching the deep fascia using a curved clamp. Build a subcutaneous tunnel above the deep facia from the precordial area to the left cervical region with a straight clamp.
10. Pull the terminal pin of the lead through the tunnel to the left cervical region using a straight clamp. Cover the terminal pin with an insulation sleeve, which is ligated using 2-0/T sutures. Suture the lead around the sleeve to the fascia and locally embed the lead at left side of neck.
11. Close the subcutaneous tissue and skin of both the thoracic and cervical incisions using 0-sutures.
12. Stop the anesthesia induction, when the animal is taking spontaneous breaths, disconnect the endotracheal tube from the ventilator. After the animal recovers from anesthesia, remove the tracheal intubation and venous catheter. Keep the animal under observation till full recovery.
13. Inject intramuscularly 800,000 U of penicillin every 12 h for 2 weeks after operation.

3. RA and RV Pacing Electrodes Implantation

1. Implant RA and RV pacing electrodes 2 weeks after LV electrodes implantation, when the animal recovers from the thoracotomy. Carry out the operation in the cardiac catheterization surgery room equipped with a fluoroscopy apparatus.
2. Induce anesthesia as in step 1.1. Secure the limbs to the operation table and maintain the animal in a supine position. Pre-medicate the animal with 0.3 g levofloxacin intravenously guttae.
3. Clip the hair of limb extremities. Connect the ECG monitor lead wires to the skin electrodes and paste the skin electrodes to limb extremities. Turn on the ECG monitor and select lead II for intra-procedural monitoring.
4. After shaving the hair of the neck, sterilize the left cervical region with iodophor and drape the sterile sheet. Administer fentanyl by a continuous rate infusion (0.01 mg/kg/hr) intravenously during the whole procedure.
5. **Venous approach**
    1. Make a small vertical incision close to the preceding wound on the left side of cervical area. Using blunt dissection, separate the fascia to expose the left external jugular vein. Separate the vein from connective tissues carefully with a mosquito clamp.
    2. Gently pull the vein up using a curved clamp and pass two 2-0/T sutures below the vein. Tie off the distal suture.
    3. Lift the distal suture gently and cut a small hole just at the middle of the two sutures with iris scissors. Using a vein pick, insert passive J-shaped RA lead and active RV lead into the left external jugular vein.

6. **RV lead implantation**
    1. Once the RV lead has been advanced to the low right atrium or inferior vena cava under fluoroscopy, withdraw the straight stylet from the RV lead. Form a J shape at the distal part of the stylet and insert it again through the RV lead.
    2. With the help of the curved stylet, introduce the lead across the tricuspid valve and into the outflow tract. Slowly withdraw both the lead and the stylet, allowing the lead tip to prolapse toward the RV apex.
    3. Replace the curved stylet with a straight one. Advance the lead towards the apex.
    4. Test the lead parameters with the stylet withdrawn about halfway. Satisfactory parameters include a pacing threshold <1.0 V at 0.48 ms, R-wave amplitude >5.0 mV, and lead impedance <2,000 Ω. Once acceptable electrical parameters are obtained, extend the active helix, remove the stylet, and re-measure the parameters.

7. **RA lead implantation**
    1. Keeping the RA lead directed toward the high anterior atrium, slowly withdraw the straight stylet, allowing retraction of the preformed J-shaped lead with its tip entering the appendage. A characteristic to-and-fro motion of the electrode with atrial activity may be observed.
    2. Satisfactory parameters include a pacing threshold <1.0V at 0.48 ms, P-wave amplitude >2.0 mV, and lead impedance <2,000 Ω. Similarly, when acceptable parameters are obtained, adjust the lead slack and remove the stylet.

8. After checking on the stability of both leads, tighten the suture proximal to the venotomy. Tie down both leads to the underlying deep fascia with two or three 2-0/T sutures around the suture sleeves. Recheck the electrical parameters and position of both leads under fluoroscopy after suturing.
9. Make a pulse generator pocket near the venous entry and in a plane just above the fascial layer and below the subcutaneous fat. Create the pocket using blunt dissection with a curved clamp. It should be just large enough to accommodate both the generator and redundant leads.
10. Clean and dry the lead pins. Cover the terminal pin of the atrial lead with an insulation sleeve and suture the lead to the floor of the pocket. Insert the ventricular lead into a pacemaker pulse generator and tighten it with the distal connector pin past the set-screws of the generator.
11. Place the generator into the pocket with the redundant leads coiling beneath the device. Tie the generator down to the fascia with a 2-0/T suture through the tie-down hole in the header of the generator. Perform the fluoroscopic examination of the entire system.
12. After checking for hemostasis, close the pocket and superficial fascia in layers using 2-0/T sutures. Finally approximate the skin edges with 0-sutures and program the pacemaker to an OVO mode using a telemetry wand.
13. For the animals of the sham group, implant the LV, RV, and RA leads in similar manner, but with no generator insertion.

4. LBB Ablation

1. Carry out the catheter ablation under the guidance of fluoroscopy immediately after RV and RA lead implantation. Shave the hair of the chest, back, and right inguinal region. Keep the animal in a supine position.
2. Prepare a multi-channel electrophysiological recorder for simultaneous surface and intracardiac electrogram recording, with filter settings of 30-400 kHz (bipolar) or 0.05-500 kHz (unipolar), and a signal amplification of 5,000 fold. Attach the cordless return electrode to the back, and the standard 12-lead electrodes to limbs and chest. Connect all leads to the electrophysiological recorder and record the electrogram at a 100 mm/s sweep speed.
3. **Venous and arterial approach**
    1. After routine disinfection and draping in the right inguinal region, make a small incision vertically through the skin. Using blunt dissection, separate the fascia to identify the right femoral vein and femoral artery.
    2. Gently pull the femoral vein up and place two stay sutures (2-0/T suture) under the vein. Tie off the vein at the distal end. Perform the same maneuver on the femoral artery.
    3. Slightly pick up the femoral vein and introduce a micropuncture needle proximally into the vein between the two sutures. Hold the needle steady and insert a flexible-tip (floppy J-shaped) guidewire through the needle.
    4. When enough guidewire has been passed into the vein, withdraw the needle and advance a dilator and sheath combination (6-Fr) over the guidewire into the femoral vein. Remove the guidewire and dilator with the sheath remaining for catheter introduction. Tie a loose suture around the vein proximal to the venotomy with the venous sheath in place.
    5. Similarly, insert a 7-Fr sheath into the femoral artery. Deliver a bolus of 100 U/kg saline-diluted heparin into the arterial sheath to prevent clotting.

4. **Mapping of right-sided His bundle potential**
    1. Advance a 6-Fr steerable quadripolar catheter into the femoral vein via the venous sheath. Connect the end of the catheter to the multi-channel electrophysiological recorder via the catheter input module by cables.
    2. Pass the catheter into the right atrium and across the tricuspid valve until it is clearly in the right ventricle. In a right anterior oblique (RAO) 30° fluoroscopy view, withdraw the catheter across the tricuspid orifice until an atrial potential appears and becomes larger. A slight clockwise torque helps to keep the electrodes in contact with the septum. When the atrial and ventricular potentials are approximately equal in size, a biphasic or triphasic deflection appears between them, representing the right-sided His bundle potential.

5. **Left bundle branch potential (LBP) mapping and ablation**
    1. Introduce a 7-Fr 4 mm-tip steerable ablation catheter into the femoral artery via the arterial sheath. Connect the end of the ablation catheter to the RF generator and multi-channel electrophysiological recorder by cables.
    2. Pass the arterial catheter retrogradely across the aortic valve and advance to the LV in an RAO 30° view. Deflect the catheter tip toward the interventricular septum. Keep the electrode in close contact with the septum.
    3. In a left anterior oblique (LAO) 45° fluoroscopy view, slowly withdraw the catheter along the septum until the left-sided His bundle potential is recorded between atrial and ventricular electrogram, just below the aortic valve. Then slowly advance the catheter along the septum and manipulate the tip to identify a discrete LBP, which is recorded beneath the aortic valve, typically 1-1.5 cm inferior to the left-sided His bundle recording site.
    4. When the potential-to-ventricular electrogram interval is about 10 ms shorter than the HV interval and an A/V electrogram ratio of <1:10 is observed, the LBP is identified. Usually the LBP to the earliest ventricular electrogram interval (LBP-V) is shorter than 20 ms, which could minimize the risk of complete A-V block.
    5. Once a satisfying LBP position is achieved, commence catheter ablation with an RF generator, delivering 500 kHz unmodulated sine-wave energy (power range 30-40 W). Adjust the power to achieve a target temperature of 60 °C at the electrode-tissue interface. If the temperature does not rise above 50 °C within 15 s, discontinue energy delivery, adjust the catheter tip, and start again.
    6. Monitor the impedance continuously during the energy application. A drop in impedance greater than 6-8 Ω during the energy delivery is considered a sign of good tissue contact and adequate heating.
    7. Typical LBBB is defined by: a prolongation of QRS duration; QRS positive in leads I, II, V5, V6 with notched R wave and negative in leads aVR, V1; and a loss of LBP electrogram. If there is no change in QRS morphology after 10 s, stop the energy delivery and adjust the catheter to find a new LBP target. When a typical LBBB QRS morphology appears on the surface electrogram, continue the energy application for 60-90 s or until a sudden rise in impedance.
    8. Stop the energy delivery immediately in the case of complete (3rd degree) atrioventricular block or ventricular fibrillation (VF). Implement electrical defibrillation rapidly whenever VF occurs.
    9. When an LBBB QRS morphology is achieved, observe the surface electrogram for a stabilization period of 30 min. If a normal QRS morphology reappears, repeat the above-mentioned ablation procedure.

6. Once the catheter ablation procedure is complete, remove both catheters. Remove the venous and arterial sheath and make tight knots rapidly on the proximal sutures to prevent hemorrhage.
7. After careful examination to preclude active bleeding, close the fascia in layers using 2-0/T sutures. Finally close the skin with 0-sutures.
8. Disconnect all electrodes from the animal and monitor the animal frequently until full recovery from anesthesia. Inject intramuscularly 800,000 U of penicillin every 12 h for 1 week after operation.
9. LBB ablation is not performed for the sham group.

5. Rapid Pacing for HF Induction

1. When the animal recovers from the operation, record the surface ECG again to confirm a permanent LBBB presence 1 week later. Then program the pacemaker to a VVI mode at 260 beats per minute (bpm) using a telemetry wand.
2. Induce anesthesia (as in step 1.1) and program the pacemaker to OVO mode after 4 weeks of rapid pacing.

Copyright © 2017 Journal of Visualized Experiments

3. Perform echocardiography to assess LVEF (with reference to step 1.4). If the LVEF decreases below 35%, prepare the animal for CRT performance. If the LVEF is still above 35%, submit the animal to rapid RV pacing again by reprogramming the pacemaker to VVI mode at 260 bpm.
4. Perform echocardiography every 2 weeks until the LVEF is below 35%. Once achieving the LVEF target, terminate rapid RV pacing and prepare for CRT strategy.
5. Animals of sham group are not submitted to rapid pacing.

6. Cardiac Resynchronization Therapy Performance

1. Divide the animals with HF into the control group and CRT group randomly. For the HF control group, let the animal survive another 8 weeks with no intervention. For CRT group, start CRT performance via biventricular pacing.
2. After anesthesia induction (as in step 1.1), keep the animal in a supine position by securing the limbs to an operation table. Pre-medicate the animal with 0.3 g levofloxacin intravenously guttae. Shave the hair of the neck, sterilize the left cervical region, and drape the sterile sheet.
3. After administering fentanyl by a continuous rate infusion (0.01 mg/kg/hr) intravenously, make a small vertical incision immediately next to the previous wound on the left side of neck. Using blunt dissection, separate the fascia to isolate the pulse generator and pacing leads (including the RV, LV, and RA leads) with no injury.
4. Disengage the terminal pin of RV lead from the generator header by loosening the screws. Carefully cut the sutures tightened on the LV and RA leads and uncap the terminal pins. Clean the pins of all leads by immersing in ethanol and using dry gauze successively.
5. Insert the RA, RV, and LV leads correctly into the header of a CRT pulse generator and tighten the screws. Enlarge the pocket using blunt dissection to be fit for the new generator. Place the generator into the pocket and tie the generator down to the floor of the pocket with a 2-0/T suture.
6. Check the pocket for hemostasis. Close the pocket and superficial fascia in layers using 2-0/T sutures. Then close the skin with 0-sutures.
7. Program the pacemaker to a DDD mode with atrioventricular (AV) delay set to a value of 70 ms and interventricular (VV) delay of 0 ms. Examine the animal frequently until recovery from anesthesia. Inject 800,000 U of penicillin intramuscularly every 12 h for 1 week.
8. After 8 weeks of CRT performance, perform the transthoracic echocardiography again on animals of all groups (as in step 1.4).

7. Sacrifice Animals and Histological Analysis

1. Secure the limbs of the animal to the operation table under general anesthesia. Inject 100 mg/kg of intravenous pentobarbital to perform animal sacrifice. Ensure animal death by absence of heart beat and breathing movement.
2. Incise the skin of the left cervical region. With a combination of sharp and blunt dissection, free the generator and the leads. Disconnect all leads from the generator by loosening the screws.
3. Free the leads from subcutaneous tissue gradually and trace them until the venous entry point. Identify the suture sleeves and cut all retention sutures. Retract the active fixation helix of the RV lead to facilitate removal.
4. Make a transverse incision at the fourth intercostal space from the sternal line to the left midclavicular line. Free the LV lead from the precordial fascia, along the subcutaneous tunnel, until the left cervical region, with a straight clamp.
5. After blunt dissection of the thoracic muscles, open the left pleural cavity. Place a rib retractor into the intercostal space. Open the pericardium completely.
6. Cut the suture on the epicardial LV lead electrode. Separate the electrode from the heart by cutting off a small piece of myocardial tissue wrapping around the electrode.
7. Cut open the right chambers along with the septum. Detach the RA and RV electrodes from myocardium using both sharp and blunt dissection. Usually the electrode tips are encapsulated by fibrous and myocardial tissues. Cut the surrounding tissues from the heart if necessary.
8. Pass a straight stylet to the tip of each lead through the terminal pin. Extract the RV and RA leads from the venous entry and remove the LV lead from the subcutaneous tunnel. If the leads cannot be extricated due to fibrous adhesions, strip away the fibrous adhesions along the leads with blunt dissection.
9. Pull the heart up gently, and clip through the heart tissue close to the aorta to excise the heart. Place the heart in a sterile bowl and rinse it several times with physiological saline. Slice the transmural myocardium from the lateral LV wall for histological analysis.
10. Fix myocardial tissues with buffered formalin, then dehydrate, and embed in paraffin. After cutting into 5 μm thick sections, deparaffinize the samples and stain with hematoxylin and eosin (HE) and Masson trichrome.
11. Measure the cellular diameters from the longitudinal sections stained with HE. Express CVF as percentage of collagen-stained area divided by total tissue area in Masson trichrome-stained sections. Select and count five high-powered fields (400x) randomly for each section. Take digital photographs and analyze using a high-resolution digital image analysis system.

Representative Results

Successful LBB Ablation:

Figure 2 represents a typical surface and intracardiac electrogram in the course of catheter ablation. The mean LBP-V measured is 18.8 ±2.8 ms, which was about 10 ms shorter than the baseline H-V interval (28.8 ±2.6 ms, p <0.01). The QRS duration prolonged from 59.2 ±6.8 ms to 94.2 ±8.6 ms (p <0.01) after LBB ablation. The loss of the LBP electrogram confirmed successful LBB ablation.

A Chronic Dyssynchronous CHF Model and CRT Benefits Quantified by Echocardiography:

Baseline echocardiographic parameters showed no significant difference among the sham, HF control, and CRT groups. As was published in our previous data[10], an obvious deteriorated cardiac function characterized by increased LVEDV and LVESV, and decreased LVEF could be observed in the HF control group at the end of the experiment (**Figure 3**). CRT improved cardiac function with decreased LVEDV and LVESV, and increased LVEF. For speckle tracking analysis, tri-plane apical longitudinal views including A4C, A2C, and APLAX were acquired simultaneously. After tracing each apical view, the longitudinal strain curves of six segments from each plane were obtained. Then the TTP and PSD were calculated. As a result, an increased asynchrony index (PSD) was induced in the HF control group compared with the sham group (51.6 ±5.9 ms *vs.* 32.6 ±2.3 ms, p <0.01); while CRT corrected LV asynchrony, as exhibited by a significantly lower PSD (44.0 ±4.6 ms *vs.* 51.6 ±5.9 ms, p <0.05). Furthermore, the HF control animals presented a significantly lower aVTI than the sham group (8.09 ±1.19 cm *vs.* 14.53 ±2.38 cm, p <0.01), which was significantly increased in the CRT group (10.92 ±1.31 cm *vs.* 8.09 ±1.19 cm, p <0.05) (**Figure 3** and **Figure 4**).

Histologic and Cellular Reverse Remodeling Induced by CRT:

Myocardial tissues excised from the LV lateral wall were subjected to histologic analysis. Compared with the sham group, a remarkably decreased cardiomyocyte diameter was noted in the HF control group (4.77 ±0.86 μm *vs.* 7.68 ±1.25 μm, p <0.01), which might be responsible for the LV dilation. Masson trichrome staining revealed a significant increase of CVF in the HF control group in contrast with the sham group (12.56 ±2.10% *vs.* 1.88 ±0.23%, p <0.01). However, 8 weeks of CRT performance resulted in a significant restoration of cardiomyocyte diameter (6.26 ±0.93 μm *vs.* 4.77 ±0.86 μm, p <0.01) and CVF (6.28 ±1.61% *vs.* 12.56 ±2.10%, p <0.01) compared with the HF control group, indicating a biologic reverse remodeling invoked by CRT (**Figure 5**).

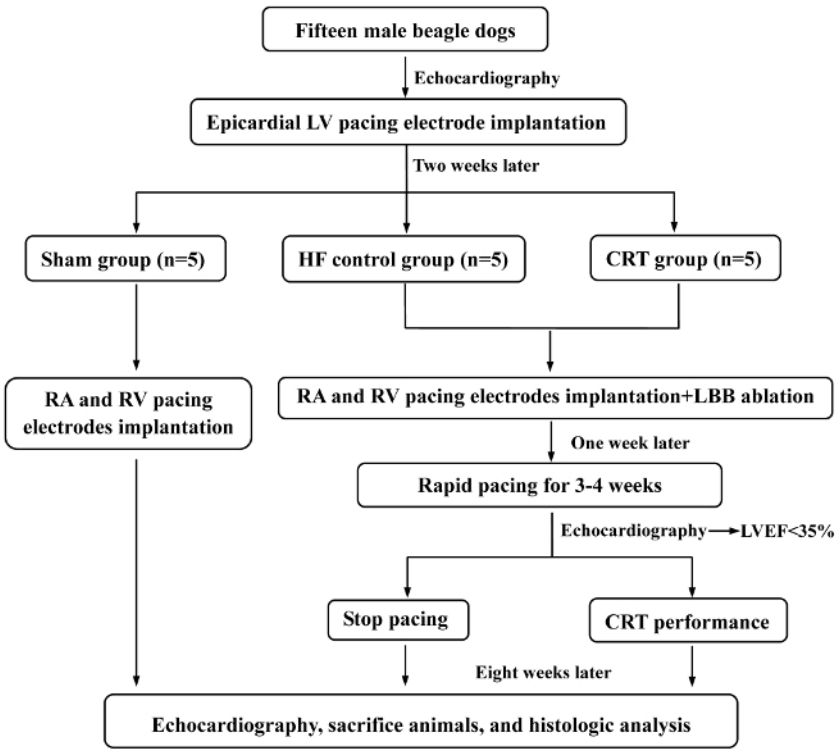

Figure 1: The schematic workflow of all protocol steps. Please click here to view a larger version of this figure.

Figure 2: 12-lead ECG and intracardiac electrogram recorded before (**A**) and after (**B**) catheter ablation. (**A**) Typical surface and intracardiac electrogram at a successful ablation site. Right-sided His bundle potential was mapped by the distal electrode of the quadripolar catheter with an H-V interval of 28 ms. The LBP was mapped by the ablation catheter with an LBP-V interval of 17 ms. The LBP-V interval was 11 ms shorter than the H-V interval. (**B**) Typical LBBB morphology after successful ablation. The QRS duration prolonged from 63 ms to 95 ms after LBB ablation, which was positive in leads I, aVF, V6, with notched R wave, and negative in lead V1. The LBP disappeared and the right-sided His bundle potential still existed after ablation. Please click here to view a larger version of this figure.

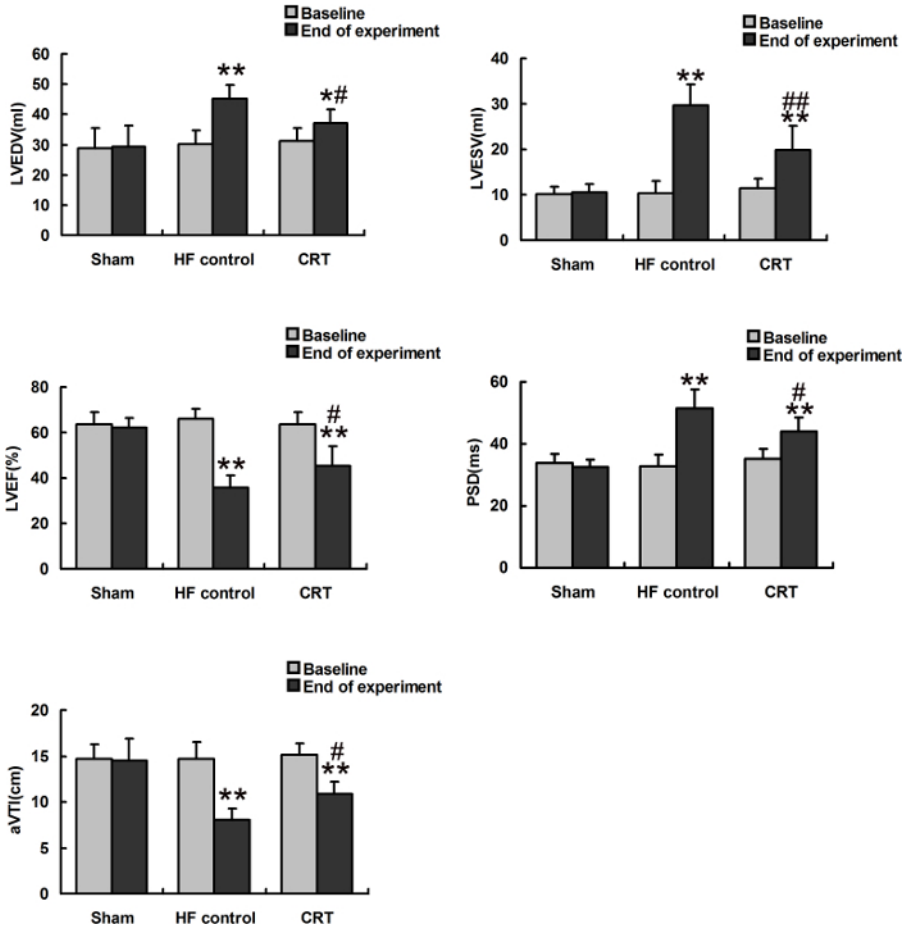

Figure 3: Bar graphs expressed as mean ± SD for LVEDV, LVESV, LVEF, PSD, and aVTI among the three experimental groups (n = 5 for each) at baseline and the end of experiment, respectively. Values between the experimental groups were compared using one-way ANOVA test. Compared with the sham group, *p <0.05, **p <0.01; Compared with the HF control group, $^{\#}p$ <0.05, $^{\#\#}p$ <0.01. Please click here to view a larger version of this figure.

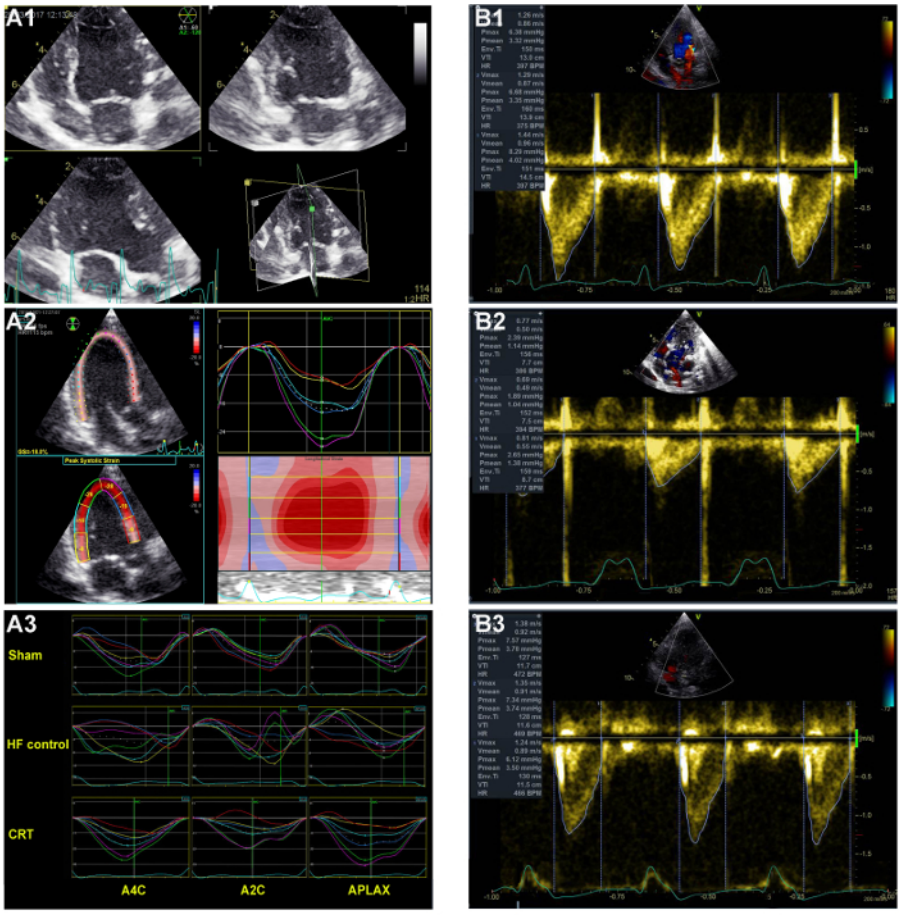

Figure 4: Speckle tracking strain imaging and aortic velocity time integral measurement. (**A**) Two-dimensional longitudinal strain analysis using speckle tracking imaging from 3 standard apical views. A1 showed tri-plane apical longitudinal views acquired using 4VD transducer of GE VIVID E9. Images were carefully adjusted to ensure that apical four chamber view (A4C), two chamber view (A2C), and long axis view (APLAX) were displayed at the same time. A2 displayed an example of longitudinal strain curves of six segments created by a tracking algorithm from APLAX view. Segments of basal-posterior wall, mid-posterior wall, apical-posterior wall, basal-anterior septum, mid-anterior septum and apical-anterior septum were automatically defined. A3 showed the time to peak longitudinal strain (TTP) of each segment calculated with QRS onset as a reference when all the segmental time-strain curves were constructed from the three apical views. A significantly higher dispersion of TTP could be observed in the HF control group, which was formulated as standard deviation. CRT performance significantly reduced the difference between TTP of each segment. (**B**) Assessment of aortic velocity time integral averaged from 3 consecutive beats. B1, B2, and B3 represent typical images of the sham group, HF control group, and CRT group, respectively. Please click here to view a larger version of this figure.

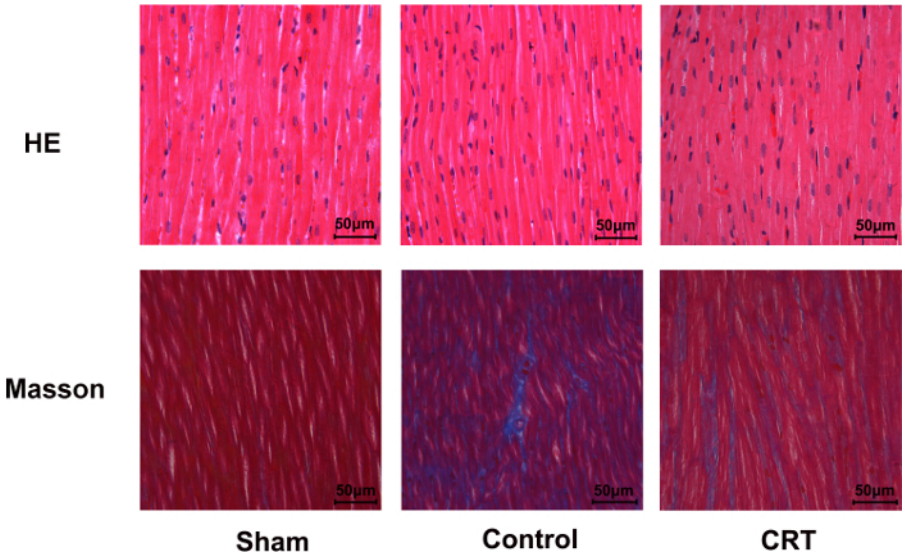

Figure 5: Typical photograph of the HE staining (400X) and Masson's trichrome staining (400X). Diameters of myocardial fibers were measured from longitudinally cut sections, and collagen volume fraction (CVF) was assessed from the percentage of fibrotic area divided by total tissue area. Scale bars = 50 μm. Please click here to view a larger version of this figure.

Discussion

Dilated cardiomyopathy constitutes a major cause of CHF, which is characterized by ventricular dilation, systolic dysfunction with reduced LVEF, and abnormalities of diastolic filling[11]. Since chronic tachycardia-mediated HF is a recognized clinical condition, rapid pacing of either atrium or ventricle for at least 3 to 4 weeks serves as a frequently used animal model to induce CHF[11]. Hemodynamic changes occur as soon as 24 h after rapid pacing, with continued deterioration of cardiac function for up to 3 to 5 weeks. However, the recovery from pacing-induced HF is a dramatic and unique feature of this model, accompanied by a reversal of neurohormonal activation, indicating a reversible nature of this myopathy. It is documented that LVEF shows significant recovery within 1 to 2 weeks after termination of pacing and nearly all hemodynamic variables return towards normal levels at 4 weeks after cessation of rapid pacing[12]. Hence, the prevention of cardiac function recovery on the discontinuation of pacing is of great importance in this attractive model.

LBBB could result in delayed LV activation and a corresponding delayed LV systole. Asynchronous contraction of the septum and the LV free wall performs a disproportionate amount of net myocardial work, and the work is wasted in both regions. Though a mere LBBB produces a low-grade myopathy, the synergy between HF and LBBB may produce substantial functional and clinical decline over time, which could be ameliorated by CRT. The functional LBBB induced by RV pacing is temporary, which is very different from the case where an anatomical LBBB is present. In the present study, a permanent LBBB was created by catheter ablation and its presence was confirmed during the subsequent experiments. Canines have a relatively longer, more left side oriented penetrating bundle of His and common left bundle, which may account for the high success rate of LBB ablation. LBP is located between His bundle and Purkinje potentials. Correct identification of LBP and a guarantee of A:V electrogram ratio <1:10 favors successful LBB ablation and avoidance of complete A-V block[13]. The common left bundle is divided into anterior and posterior fascicles at the proximal one-thirds along the muscular ventricular septum. If the ablation catheter is positioned on a distal portion of the bundle branch, an anterior or posterior fascicle might be ablated. However, the ablation of these fascicles could not obviously prolong the QRS duration. Based on a previous study, the QRS duration could increase by 40-50 ms following LBB ablation[13]. In the present study, the QRS prolongation averaged 35 ms, which might be due to different animal species. On intracardiac electrogram, the mean LBP-V interval for successful ablation measured about 16-19 ms, usually 10 ms shorter than the H-V interval, neither too close nor too far from the His bundle. In addition, the LBP usually disappeared after successful ablation[14].

A previous study has reported that rapid pacing for at least 3 to 4 weeks produces a reliable and reproducible HF model[11]. There may exist some difference among different animals as for the necessary period of tachypacing. So, echocardiography was performed every 2 weeks during rapid pacing. None of the animals showed an LVEF <35% after 2 weeks of tachypacing, suggesting that 3 to 4 weeks of rapid pacing is essential. After 4 weeks, once the LVEF was below 35%, rapid pacing was terminated. Such a strategy helped to uniform the baseline HF severity. In addition, since RV apical (RVA) pacing has long been proven to induce LV dyssynchrony and HF[15], we selected RVA instead of RA for rapid pacing. Thus, rapid pacing-induced HF with superimposed LBBB-induced dyssynchrony in our study helped to establish a model of stable and chronic dyssynchronous HF. More importantly, the LV systolic dysfunction hardly recovered in up to 8 weeks of observation in the control group. Such an animal model favored investigation of CRT benefits instead of self-recovery.

To establish the HF model, first we implanted the LV epicardial lead via left thoracotomy. After 2 weeks of recovery from thoracotomy, we implanted the RV and RA leads via a jugular vein approach, followed by LBB ablation. Although limited left thoracotomy, muscle sparing, and rib preservation strategies are excellent minimally invasive approaches for exposure of the LV lateral wall, operative trauma and postoperative infection are still associated with high mortality. So, the LV lead implantation was performed before other procedures. Only those surviving 2 weeks after the operation are submitted to LBB ablation and rapid pacing. Overall, this was an economical strategy.

Echocardiographic data demonstrated persistence of significant systolic dysfunction, increased ventricular volumes, and higher asynchrony index in our CHF model. CRT improved cardiac function with reduced asynchrony index. Speckle tracking strain analysis is a novel method which permits the assessment of myocardial deformation. It has proven to be significantly associated with long-term outcome after CRT and

has additive prognostic value to routine selection criteria for CRT. Of the three different patterns of myocardial deformation including radial strain, circumferential strain, and longitudinal strain, it is still under debate with conflicting data, which one used for LV dyssynchrony index may best predict CRT response[16,17]. However, it is reported that global longitudinal strain consistently showed good reproducibility, while reproducibility was moderate for circumferential strain and poor in the radial direction[18]. Therefore, in the present study, we adopted the apical tri-plane longitudinal strain analysis as the LV asynchrony index by calculating PSD. A higher PSD indicated a severer asynchrony. aVTI has been commonly used for AV and VV delay optimization in CRT patients. Changes in aVTI can serve as a surrogate for changes in stroke volume as it is directly proportional to the LV outflow tract VTI[19]. Hence, we assessed aVTI to evaluate hemodynamic benefits from CRT. A higher aVTI suggested better LV systolic performance.

Cardiac fibrosis, as characterized by interstitial collagen and extracellular matrix deposit, is a hallmark of end-stage CHF. Recent studies have demonstrated that LV reverse remodeling after CRT is independently associated with diffuse interstitial myocardial fibrosis, which is assessed with myocardial T1 mapping cardiac magnetic resonance (CMR)[20]. Besides, CRT-induced LV reverse remodeling is also associated with a decreased plasma level of pro-fibrotic cytokines such as transforming growth factor (TGF)-β_1 and osteopontin (OPN)[21,22]. In the present study, histologic analysis revealed decreased cardiomyocyte diameter and increased myocardial fibrosis in the failing heart at 8 weeks after cessation of rapid pacing, suggesting a histologic and cellular remodeling in our HF model. Along with the structural reverse remodeling, however, CRT restored myocyte configuration and alleviated collagen deposits. Such a histologic reverse remodeling yields more beneficial effects beyond CRT itself.

Recent recommendations for CRT implantation include persistent HF symptoms, impaired LV systolic function with LVEF ≤35%, LBBB QRS morphology, and a widened QRS duration[4]. Our experimental model is a practicable, reproducible, and stable HF model, which satisfies almost all these criteria. While it is noteworthy that our work established a canine model of non-ischemic dilated cardiomyopathy, it may not apply to other conditions such as valvular heart disease, congenital heart disease, ischemic HF, *etc*. Especially, coronary ligation or microembolization is commonly used to produce ischemic HF, which has a higher risk of sudden cardiac death. However, due to the discrepancy of myocardial scar burden in ischemic HF, it is not easy to objectively evaluate CRT benefits. By contrast, our experimental model is relatively homogeneous and is a suitable model for studying CRT performance, including electrical behavior, echocardiographic assessment, and biologic and molecular modifications.

Disclosures

The authors declare that they have no competing financial interests.

Acknowledgements

This work is funded by National Natural Science Foundation of China (81671685) and Shanghai Commission of Health and Family Planning (No. 201440538)

References

1. Bristow, M.R. *et al.* Cardiac-resynchronization therapy with or without an implantable defibrillator in advanced chronic heart failure. *N Engl J Med.* **350**(21), 2140-2150 (2014).
2. Cleland, J.G. *et al.* The effect of cardiac resynchronization on morbidity and mortality in heart failure. *N Engl J Med.* **352**(15), 1539-1549 (2005).
3. Rickard, J. *et al*. Predictors of response to cardiac resynchronization therapy: A systematic review. *Int J Cardiol.* **225**, 345-352 (2016).
4. Ponikowski, P. *et al.* 2016 ESC Guidelines for the diagnosis and treatment of acute and chronic heart failure: The Task Force for the diagnosis and treatment of acute and chronic heart failure of the European Society of Cardiology (ESC). Developed with the special contribution of the Heart Failure Association (HFA) of the ESC. *Eur J Heart Fail.* **18**(8), 891-975 (2016).
5. Yang, S. *et al.* Glycoproteins identified from heart failure and treatment models. *Proteomics.* **15**(2-3), 567-579, (2015).
6. Barth, A.S. *et al.* Cardiac resynchronization therapy corrects dyssynchrony-induced regional gene expression changes on a genomic level. *Circ Cardiovasc Genet.* **2**(4), 371-378 (2009).
7. Howard, R.J., Stopps, T.P., Moe, G.W., Gotlieb, A., & Armstrong, P.W. Recovery from heart failure: structural and functional analysis in a canine model. *Can J Physiol Pharmacol.* **66**(12), 1505-1512, (1988).
8. Vernooy, K. *et al.* Cardiac resynchronization therapy cures dyssynchronopathy in canine left bundle-branch block hearts. *Eur Heart J.* **28**(17), 2148-2155 (2007).
9. Spragg, D.D., & Kass, D.A. Pathobiology of left ventricular dyssynchrony and resynchronization. *Prog Cardiovasc Dis.* **49**(1), 26-41, (2006).
10. Wang, J. *et al.* Effect of Cardiac Resynchronization Therapy on Myocardial Fibrosis and Relevant Cytokines in a Canine Model With Experimental Heart Failure. *J Cardiovasc Electrophysiol.* **28**(4), 438-445 (2017).
11. Houser, S.R. *et al.* Animal models of heart failure: a scientific statement from the American Heart Association. *Circ Res.* **111**(1), 131-150 (2012).
12. Shinbane, J.S., Wood, M.A., Jensen, D.N., Ellenbogen, K.A., Fitzpatrick, A.P., & Scheinman, M.M. Tachycardia-induced cardiomyopathy: a review of animal models and clinical studies. *J Am Coll Cardiol.* **29**(4), 709-715, (1997).
13. Helguera, M.E., Trohman, R.G., & Tchou, P.J. Radiofrequency catheter ablation of the left bundle branch in a canine model. *J Cardiovasc Electrophysiol.* **7**(5), 415-423, (1996).
14. Blanck, Z., Deshpande, S., Jazayeri, M.R., & Akhtar, M. Catheter ablation of the left bundle branch for the treatment of sustained bundle branch reentrant ventricular tachycardia. *J Cardiovasc Electrophysiol.* **6**(1), 40-43 (1995).
15. Auger, D. *et al.* Effect of induced LV dyssynchrony by right ventricular apical pacing on all-cause mortality and heart failure hospitalization rates at long-term follow-up. *J Cardiovasc Electrophysiol.* **25**(6), 631-637 (2014).

Copyright © 2017 Journal of Visualized Experiments

16. Delgado-Montero, A. *et al.* Additive Prognostic Value of Echocardiographic Global Longitudinal and Global Circumferential Strain to Electrocardiographic Criteria in Patients With Heart Failure Undergoing Cardiac Resynchronization Therapy. *Circ Cardiovasc Imaging.* **9**(6), pii: e004241 (2016).
17. Delgado, V. *et al.* Assessment of left ventricular dyssynchrony by speckle tracking strain imaging comparison between longitudinal, circumferential, and radial strain radial strain in cardiac resynchronization therapy. *J Am Coll Cardiol.* **51**(20), 1944-1952 (2008).
18. Risum, N. *et al.* Variability of global left ventricular deformation analysis using vendor dependent and independent two-dimensional speckle-tracking software in adults. *J Am Soc Echocardiogr.* **25**(11),1195-1203 (2012).
19. Barold, S.S., Ilercil, A., & Herweg, B. Echocardiographic optimization of the atrioventricular and interventricular intervals during cardiac resynchronization. *Europace.* **10**(Suppl 3),iii88-iii95, (2008).
20. Höke, U. *et al.* Relation of Myocardial Contrast-Enhanced T1 Mapping by Cardiac Magnetic Resonance to Left Ventricular Reverse Remodeling After Cardiac Resynchronization Therapy in Patients With Nonischemic Cardiomyopathy. *Am J Cardiol.* **119**(9),1456-1462 (2017).
21. Osmancik, P., Herman, D., Stros, P., Linkova, H., Vondrak, K., & Paskova, E. Changes and prognostic impact of apoptotic and inflammatory cytokines in patients treated with cardiac resynchronization therapy. *Cardiology.* **124**(3), 190-198 (2013).
22. Francia, P. *et al.* Plasma osteopontin reveals left ventricular reverse remodelling following cardiac resynchronization therapy in heart failure. *Int J Cardiol.* **153**(3), 306-310 (2011).

Copyright © 2017 Journal of Visualized Experiments